This document is the accepted manuscript version of the following article:Tayebzadeh Moghadam, N., Abbaspour, K. C., Malekmohammadi, B., Schirmer, M., & Yavari, A. R. (2021). Spatiotemporal modelling of water balance components in response to climate and landuse changes in a heterogeneous mountainous catchment. Water Resources Management. https://doi.org/10.1007/s11269-020-02735-w

Spatiotemporal Modelling of Water Balance Components in Response to Climate and Land Use Changes in a Heterogeneous Mountainous Catchment

Negar Tayebzadeh Moghadam [1,2] • Karim C. Abbaspour [3] • Bahram Malekmohammadi [1] • Mario Schirmer [2,4] • Ahmad Reza Yavari [1]

[1] School of Environment, College of Engineering, University of Tehran, Tehran, Iran
[2] Eawag, Swiss Federal Institute of Aquatic Science and Technology, Department of Water Resources and Drinking Water, Duebendorf, Switzerland
[3] Eawag, Swiss Federal Institute of Aquatic Science and Technology, Department Systems Analysis, Integrated Assessment and Modelling, Duebendorf, Switzerland
[4] University of Neuchâtel, Centre for Hydrogeology (CHYN), Neuchâtel, Switzerland

Corresponding author: Bahram Malekmohammadi
E-mail address: Malekb@ut.ac.ir
Tel: +98 21 61113185; Fax: +98 21 66407719

Abstract

Land use change and climate change are the main drivers of hydrological processes. The purpose of this study was to analyse the separate and combined future effects of climate and land use changes on water balance components on different spatial and temporal scales using the integrated hydrological Soil and Water Assessment Tool model. The study focused on the changes and relationship between water yield (WYLD) and sediment yield (SYLD) in the heterogeneous Taleghan Catchment in Iran. For future climate scenarios, RCP 4.5 and RCP 8.5 of GFDL-ESM2M GCM were used for the period 2020–2040. A Markov chain model was used to predict land use change in the catchment. The results indicated an increase in precipitation and evapotranspiration. The findings also showed that the relationship between WYLD and SYLD is direct and synergic. Climate change has a stronger effect on WYLD than land use change, whereas land use change has a stronger effect on SYLD. The conversion of rangelands to barren land is the most critical land use

change that could lead to increased SYLD. The highest increase in WYLD and SYLD in scenario RCP4.5 was the result of the combined effects of climate and land use change. We estimated WYLD of about 295 mm and SYLD of around 17 t/ha. The proposed methodology is universal and can be applied to similar settings to identify the most vulnerable regions. This can help prioritize management strategies to improve water and soil management in watersheds.

Keywords Water yield • Sediment yield • SWAT model • Taleghan Catchment • Iran

1 Introduction

With the increase in the global population, water resources are becoming increasingly threatened by drivers of change that can be directly or indirectly attributed to human activity (Boretti and Rosa 2019). Land use change and climate change are the two main drivers of hydrological processes influencing the available water resources and flow regimes on various temporal and spatial scales in river basins worldwide (Dibaba et al. 2020). Climate and land use changes have a considerable impact on the water balance of a basin and its sub-basins. Water balance components (WBCs) include precipitation, evapotranspiration (ET), total runoff, surface runoff, groundwater recharge, and soil water content (Arnold et al. 2011). Land use change can affect river flow and other water cycle components, such as groundwater recharge, which can decline during the dry season due to reduced infiltration (Chauhan et al. 2020). Reduced groundwater recharge and soil water content can reduce ET (Seyoum et al. 2015). Climate variations can also affect ET, soil moisture, temperature, precipitation patterns, humidity, and flow routing times (Ramteke et al. 2020).

The quantification of various components in a watershed remains challenging (Ning et al. 2015). Many studies have dealt with one particular component of the water balance,

such as streamflow (Nilawar and Waikar 2019), groundwater recovery (Ni et al. 2020), runoff (LV et al. 2020), ET (Chen et al. 2020), or a particular phenomenon or parameter throughout a year, such as low flows, peak flows (Aparicio et al. 2019), and soil moisture (Uniyal et al. 2020). Fewer studies have focused on the relationship between water yield (WYLD) and sediment yield (SYLD) on different spatial and temporal scales (Schmalz et al. 2016; Tian et al. 2016).

Several studies have analysed the individual or combined effects of climate and land use changes on catchments' WBCs. Kundu et al. (2017) investigated future WBCs by applying a Soil and Water Assessment Tool (SWAT) model in different sub-basins, considering climate and land use changes. Their separate and combined effects on water balance showed increasing WYLD and decreasing ET in the future. Climate change alone led to higher WYLD, surface runoff, and ET. Land use change alone, on the other hand, resulted in increased WYLD and surface runoff but decreased ET. Nilawar and Waikar (2019) used a SWAT model to evaluate the impact of climate change on streamflow and sediment concentration under an emission stabilization scenario, Representative Concentration Pathway (RCP) 4.5, and a high emission scenario (RCP 8.5) at the Purna River Basin in India. They concluded that streamflow and sediment loads will likely increase significantly at the basin's outlet from June to September. Zhang et al. (2020) applied the SWAT to simulate hydrological responses to land use change in Australia. They observed a significant positive correlation between annual rainfall and total runoff for evergreen forests, range grasses, and urban land use. Evergreen forests generally produced less total runoff than range grasses and urban land use under the same rainfall conditions, terrain slope, and soil texture. Urban land use generally produced more surface runoff and less lateral runoff and groundwater recharge than evergreen forests and range grasses under the same conditions. Choukri et al. (2020) used the SWAT to examine the impacts of climate

and land use changes on water availability and sediment loads for a water supply reservoir in northern Morocco. Their results showed that climate change would significantly decrease the reservoir's annual water supply and sediment volume. The scenarios of land use change would lead to a moderate change in annual water inflow and a significant decrease in sediment transport into the reservoir. The combined effects of climate and land use changes would reduce the yearly water availability and sediment supply. Ndhlovu and Woyessa (2020) evaluated the effect of climate change on catchment water balance in the Kabompo River Basin in Zambia using a SWAT model. Their results indicated that future water balance would not change significantly under RCP 4.5, as rainfall would decrease by only 1%. WYLD and runoff would increase by 5% and 6%, respectively. Under RCP 8.5, rainfall would increase by 19%, while WYLD and runoff would increase by 40% and 65%, respectively.

Fewer studies have focused on the relationships between WBCs on different spatial and temporal scales. Such analyses are necessary for identifying the most vulnerable regions and explaining the reasons for their vulnerability (e.g., Kundu et al. 2017; Nandi and Reddy 2020; Zhang et al. 2020), especially in arid and semi-arid regions of the Middle East, such as Iran (Nasiri et al. 2020). Compared with other areas of the world, less attention has been paid to the combined effects of future climate and land use changes on water resources in Iran (Shooshtari et al. 2017). Assessing the effects of both climate and land use changes on hydrological components can significantly improve the predictability of water availability, thus helping stakeholders make more informed decisions. To predict future water balance trends, both their individual and combined effects should be considered (Kundu et al. 2017).

This study's primary objective was to assess changes in future WBCs by investigating the independent and combined effects of climate and land use changes on different spatial

and temporal scales using the integrated hydrological SWAT model. We used the SWAT because it is a time-continuous and spatially distributed watershed model successfully applied on various scales and in different environmental conditions (Gassman et al. 2007). We analysed monthly and annual WYLD and SYLD trends in the Taleghan Catchment and its sub-basins. This research aimed to provide a methodological framework for future assessment of WBCs in the study region, considering different spatial and temporal scales. We were able to determine the most critically vulnerable areas in a heterogeneous mountainous catchment. Our study improves our understanding of the synergic relationship between WYLD and SYLD by exploring various processes involved.

2 Study Area and Materials

2.1 Study Area

The Taleghan Catchment is located in the north of Iran within 36° 04′ to 36° 21′ N latitude and 50° 38′ to 51° 12′ E longitude. It covers approximately 800 km^2 and has a long-term average annual precipitation of 591 mm and an average temperature of 11.4°C. Figure 1 shows the study area, whose topographical elevation ranges between 1,779 and 4,212 m above mean sea level with a weighted average of 2,753 m (Hosseini and Ashraf 2015). Its land use consists of 85% rangeland and 15% orchards, agriculture, and other uses (Bazab Consulting Engineers 2015). The Taleghan Catchment is vital for agriculture and water supply, especially since the construction of a dam in 2006. An increasing population and demand for water and land have led to significant pressure on land and water resources in the catchment. Proper management of watersheds is one of the most critical measures for optimal use of its water and soil resources.

2.2 Materials

Land use information was obtained from the Landsat 8-OLI image acquired in 2016. Landsat 5 TM images of 1996 and 2006 with a spatial resolution of 30 m were also used (https://earthexplorer.usgs.gov/). Geometric and radiometric corrections of the images were performed using a first-order polynomial model and a root mean square error of 0.5 pixels in the geometric correction (Zheng et al. 2016; Verma et al. 2017). The images were cloud-free and allowed accurate land use classification (Wilken et al. 2017). ArcGIS 10.3 (www.esri.com) and ENVI 5.3 (www.harrisgeospatial.com) were used to classify the land use types. Ground truth data were obtained from a field investigation in a supervised land use classification and accuracy assessment of the classified results. The Crosta method provided a false colour composite image of training areas (Crosta and Moore 2007). The classification was performed using a maximum likelihood algorithm (Karan and Samadder 2016; Verma et al. 2017). Land use was classified as orchard, agricultural, good rangeland, poor rangeland, urban, and barren land (Fig. 2). Other databases used to build the SWAT model are presented in Table 1. Four hydrologic stations were used to calibrate and validate the model (Fig. 1). Hydrological stations from right to left are Gatedeh, Dehdar, Joestan, and Galinak. Galinak is the catchment outlet.

3 Methodology

The steps involved in developing the proposed methodology are presented in Fig. 3. A description is provided in sections 3.1–3.4.

3.1 Step 1: Prediction of Land Use Change

The Cellular Automata-Markov (CA-Markov) model was applied to predict land use changes using the TerrSet 18.2 (Eastman 2015). The model generates transition matrices of different years to assess land use change. The land use map of 2016 was modelled on

154 the changes between 1996 and 2006. Calibration and validation of the model were
155 performed by comparing the classified 2016 image with the model-generated image. Data
156 from 2006 to 2016 were used to model the land cover for 2040.

157 3.2 Step 2: Prediction of Climate Change

158 For the simulation of future temperature and precipitation, we used the Geophysical Fluid
159 Dynamics Laboratory's Earth System Model 2M (GFDL-ESM2M) (GCM1) during the
160 period 2020–2040 under four carbon scenarios. Observed climate datasets over 17 years
161 (2000–2016) were used as the baseline climate data. The reason for choosing the GFDL-
162 ESM2M was that it was recently developed to better understand Earth's biochemical cycle,
163 including human activity (Dunne et al. 2012). The Climate Change Toolkit was used for
164 bias correction and downscaling of GCM outputs, as well as spatial interpolation of climate
165 data. The ratio method was used for rainfall, and the additive method was used for
166 temperature (Vaghefi et al. 2017).

167 3.3 Step 3: SWAT Hydrological Model Calibration

168 The catchment was divided into 51 sub-basins in the SWAT model and further discretized
169 into 700 hydrologic response units (HRUs), representing a unique land use, soil, and slope
170 class (Arnold et al. 2011). The SUFI-2 optimization algorithm in the SWAT-CUP software
171 (Abbaspour et al. 2007) was used for model calibration and validation and for sensitivity
172 and uncertainty analysis. In SUFI-2, the uncertainty of the model input parameters is
173 depicted as uniform distributions. In contrast, output uncertainty is quantified using the
174 95% prediction uncertainty. The calibration covered the period 2002–2012 with two years
175 of warm-up simulation for model initialization. The validation covered the period 2013–
176 2016. The Nash-Sutcliffe efficiency (NSE; Nash and Sutcliffe 1970) was used as the
177 performance criterion objective function:

$$NSE = 1 - \frac{\sum_{i=1}^{n}(Q_{obs,i} - Q_{sim,i})^2}{\sum_{i=1}^{n}(Q_{obs,i} - \bar{Q}_{obs})^2} \quad (1)$$

where n is the number of observed data, $Q_{obs,i}$ is the observed streamflow during a day or month i, Q_{obs} is the average observed streamflow, and $Q_{sim,i}$ is the streamflow simulated during a day or month i. The objective function was calculated as:

$$g = \frac{1}{\sum_{j=1}^{n} w_j} \sum_{j=1}^{n} w_j \, NSE_j \quad (2)$$

where w_j is the weight of the jth variable assumed to be 1. Thus, the objective function value is the weighted average NSE of all stations.

Two types of sensitivity analyses can be performed in SWAT-CUP: one-at-a-time (OAT) and all-at-a-time (AAT). In AAT, the sensitivity of the parameters is computed using multiple regression:

$$g = \alpha + \sum_{i=1}^{n} \beta ibi \quad (3)$$

where g is the objective function value, a is the regression constant, and b is the parameters' coefficient. Moreover, the t-test and p-values are used to measure the significance of the parameters' sensitivity. The larger the absolute value of the t-test and the smaller the p-value, the more sensitive the parameter.

3.4 Step 4: Spatial and Temporal Dynamics of Water Balance Components

We simulated WBCs, WYLD, and SYLD for different land use and climate scenarios. WBCs included surface runoff, lateral flow contribution to stream, groundwater contribution to streamflow, and transmission losses (Arnold et al. 2011). For SYLD, the Modified Universal Soil Loss Equation was used in the SWAT model (Williams 1975).

4 Results

4.1 Land Use Change During 1996–2040

Land use maps for 1996, 2006, 2016, and 2040 are shown in Fig. 2. In the CA-Markov model, the overall classification accuracy for 1996, 2006, and 2016 was 94.47, 97.36, and 90.68, with kappa coefficients of 0.89, 0.96, and 0.85, respectively. In the baseline scenario of 2016, about 85% percent of the Taleghan Catchment area was covered with rangelands, of which 47% were classified as good and 38% were classified as poor (Table 2). Between 1996 and 2006, the percentage of urban land use increase was at a constant 0.28%. After the construction of the Taleghan Dam from 2006 to 2016, it increased to 0.92%. The current trend is expected to continue until 2040 by up to 1.32%. From 1996 to 2016, the rate of change was −0.32% for good rangelands and −10.24% for poor rangelands. From 2016 to 2040, 4.47% of good rangelands and 5.38% of poor rangelands are expected to disappear. Orchard lands increased by about 1.3% between 1996 and 2016 but are expected to decrease to 0.93% by 2040. Agricultural land use decreased by 0.23% between 1996 and 2016. A small growth of 0.19% is expected by 2040. The dominant trend from 1996 to 2040 is the conversion of rangeland to barren land by 10%. Barren land increased by 8.8% between 1996 and 2016 and is expected to increase by 8.3% between 2016 and 2040.

4.2 SWAT Model Calibration and Validation and Sensitivity and Uncertainty Analysis

Figure 4 shows the monthly runoff efficacy and evaluation index during calibration and validation at the Galinak station. We obtained good model calibration and validation, as indicated by several criteria for each hydrologic station (Table 3). The NSE values for sediment ranged from 0.52 to 0.58 for the calibration period and from 0.48 to 0.55 for the validation period. Sediment is generally more difficult to calibrate because of larger errors in the measurements and inconsistencies between the measured and simulated data. Manning's n-values obtained from the AAT sensitivity analysis showed that the main

channel (CH_N2), initial SCS runoff curve number for moisture condition II (CN2), and effective hydraulic conductivity in main channel alluvium (CH_K2) were the three most sensitive parameters for flow. The Universal Soil Loss Equation (USLE) support practice factor (USLE_P) was the most sensitive, followed by the peak rate adjustment factor for sediment routing in the sub-basin (ADJ_PKR) and the USLE soil erodibility factor (USLE_K). The curve number was strongly associated with the land use type. The changed land uses received the corresponding calibrated CN2 values. Moreover, higher USLE_P values were observed at Gatedeh and Dehdar, where soil erosion is high due to less vegetation and increased runoff. Crop parameters were not changed directly in the SWAT model, but they were indirectly changed by changing land use.

4.3 Separate and Combined Effects of Climate and Land Use Change on Water Yield and Sediment Yield

Six scenarios (S) for the present and future were considered in the analysis. Theses were the baseline scenario for land use 2016 and climate data 2000-2016, S1 for land use 2040 and climate data 2000-2016, S2 for land use 2016 and climate data 2020-2040 under RCP 4.5, S3 for land use 2016 and climate data 2020-2040 under RCP 8.5, S4 for land use 2040 and climate data 2020-2040 under RCP 4.5, and S5 for land use 2040 and climate data 2020-2040 under RCP 8.5.

4.3.1 Analysis of Water Balance Components

In the baseline scenario and S1, precipitation amounted to 629 mm (Table 4). The analysis of the impact of land use change on WBCs indicated an increase of 2% in WYLD (5.27 mm) and a decrease of 1% in ET (5.2 mm) by 2040. Land use change increased surface runoff by 17% and decreased groundwater recharge by 11%. Lateral flow and revap

248 (capillary flow from the shallow aquifer into the root zone) decreased by 5% and 10%,
249 respectively. The impact of climate change alone on WBCs in S2 and S3 resulted in a
250 precipitation increase of 14% (717 mm) under RCP 4.5 and 2% (641 mm) under RCP 8.5.
251 The following changes were observed in S2 and S3: surface runoff of 5% and −13%,
252 respectively; ET of 20% and 9%, respectively; groundwater recharge of 7% and −9%,
253 respectively; lateral flow of 7% and −3%, respectively; and revap of 0% and −8%,
254 respectively. Climate change increased WYLD by 7% in RCP 4.5 and decreased it by 8%
255 in RCP 8.5. SYLD increased by 447% in RCP 4.5 and 191% in RCP 8.5 compared to the
256 baseline. The maximum temperature increased by 1.29°C in RCP 4.5 and 1.81°C in RCP
257 8.5. The minimum temperature increased by 0.47°C and 0.9°C under RCP 4.5 and RCP
258 8.5, respectively. The amount of ET relative to the precipitation in RCP 4.5 was higher than
259 in RCP 8.5 due to the higher temperature (Table 4).

260 In the analysis of the combined effects of climate and land use changes on WBCs,
261 precipitation increased by 14% (717 mm), ET by 18% (422 mm), and surface runoff by
262 26% (124 mm) in S4 (Table 4). Changes of −7% in groundwater recharge, 4% in lateral
263 flow, −10% in revap, 9% in WYLD, and 17 t/ha in SYLD were observed. In S5,
264 precipitation, ET, and surface runoff increased by 2%, 6%, and 11%, respectively.
265 Groundwater recharge, lateral flow, revap, and WYLD decreased by 21%, 7%, 19%, and
266 4%, respectively. However, SYLD increased by 11.7 t/ha compared to the baseline scenario
267 (Table 4).

268 **4.3.2 Water Yield and Sediment Yield Analysis on the Basin and Sub-Basin Spatial**
269 **Scales**

270 In S1, average annual WYLD increased from 270 to 275 mm from 2016 to 2040 in the
271 entire Taleghan Catchment as a result of land use change. In 2040, the WYLD range in all
272 sub-watersheds except for sub-basins 33 and 34 was higher than or similar to the 2016

values (Fig. 5). Regions of high WYLD were mainly in sub-basins 1 and 2 and ranged between 251 and 300 mm. Annual average SYLD in 2040 was 13 t/ha, ranging from 2 to 65 t/ha, with sub-basin 1 having the highest value (Fig. 6).

In S2 and S3, average annual WYLD increased by 18 mm in RCP 4.5 and decreased by 22 mm in RCP 8.5 (Table 4). A possible reason for this could be more rainfall in RCP 4.5. In S2, the maximum WYLD occurred in sub-basins 1 and 2, ranging from 251 to 300 mm (Fig. 5). The minimum occurred in sub-basin 34, with less than 50 mm. In S3, the sub-basins with the highest and lowest WYLD values were the same as S2, except that the highest WYLD ranged from 201 to 250 mm. As shown in Fig. 6, the highest SYLD in S2 and S3 was observed in sub-basin 51, with 34 and 25 t/ha, respectively. In both scenarios, many sub-basins showed an increasing trend in SYLD relative to the baseline. However, SYLD was not as high as in S1 in the land use change analysis.

In S4, WYLD amounted to 295 mm (Table 4). In some sub-basins, such as 1 and 2, it ranged between 301 and 350 mm, whereas in others, such as sub-basin 33, it was less than 50 mm. In 22 sub-basins, WYLD was more than 201 mm. Thus, of all the scenarios, S4 showed the highest WYLD.

In S5, WYLD decreased by about 10 mm compared to the baseline scenario (Table 4). The sub-basins with high and low WYLD values were the same as those in S4 (Fig. 5). Average annual SYLD reached 17 t/ha in S4 and 12.9 t/ha in S5, that is, 14 and 11 times the baseline scenario, respectively (Table 4). As shown in Fig. 6, SYLD exhibited an increasing trend. In both scenarios, the highest SYLD was observed in sub-basin 1, ranging between 66 and 80 t/ha in S4 and between 51 and 65 t/ha in S5.

4.3.3 Annual and Monthly Water and Sediment Yields

The Taleghan Catchment is located in a hot and dry region with a high rate of ET. In both the baseline scenario and S1, spring rainfalls started at the beginning of March. With the

298 increasing temperature, the snow melted, and spring floods caused increased surface runoff.
299 As a result, WYLD rose to its highest, to 50 mm, in April (Fig. 7). With the higher
300 temperatures in summer, WYLD decreased but was maintained at 7 mm in the baseline
301 scenario and 8 mm in S1 from July to September, when rainfall was negligible. In the
302 baseline scenario, the highest SYLD was obtained in April (0.4 t/ha) and February (0.26
303 t/ha) (Fig. 8). In other months, it was negligible. In S1, SYLD increased from 0.96 t/ha in
304 January to 4.22 t/ha in April, decreased to 3.2 t/ha in May, and was close to zero in June,
305 July, and August. A gradual increase was then observed from September to January.
306 In S2, WYLD increased from 22 mm in March to 77 mm in April (Fig. 7). However,
307 from May to June, there was a sharp decrease to 19 mm. WYLD gradually declined from
308 May to September and then increased to 28 mm from September to February.
309 In S3, the WYLD trend was similar to that in S2 for the same period, it was 1–14 mm
310 less in all months. The increase in rainfall in these two scenarios was greater in spring than
311 in the cold season. The highest values of SYLD in both S2 and S3 were observed in spring
312 and winter (Fig. 8). In S2, it was 2.5 t/ha in April, 3.05 t/ha in May, and 0.56 t/ha in
313 February. In S3, it was 0.88 t/ha in April, 1.61 t/ha in May, and 0.72 t/ha in February. In
314 the other months, SYLD was insignificant in both scenarios.
315 In S4 and S5, WYLD changed somewhat compared to the base scenario but was entirely
316 following S2 and S3. It was 80 mm in May and 41 mm in April under S4 and 64 mm in
317 May and 37 mm in April under S5. In both scenarios, the highest WYLD was in spring
318 (April to May), and the lowest was in summer (June). In the cold season, February had the
319 highest WYLD. SYLD showed trends similar to WYLD in both scenarios. It increased
320 from January to May (except March) and decreased to near zero from June to January. The
321 highest amount was observed in May, with 7.27 t/ha in S4 and 4.25 t/ha in S5.

322 # 5 Discussion

Analyses of the spatial-temporal responses of WBCs to climate and land use changes are necessary for estimating future water availability and developing sustainable water management plans (Schmalz et al. 2016). In the Taleghan Catchment, a gradual decline in rangelands was observed from 1996 to 2016. Due to the conversion of mostly dryland farms to rangelands from 1996 to 2006, increasingly more local people migrated in search of better jobs. Since 2006, after the construction of the Taleghan Dam, some of the population returned, which resulted in a new decrease in the quality of rangelands.

Moreover, agricultural lands have been declining due to people's reluctance to engage in farming. These lands have been converted to residential areas. Urbanization resulted in more runoff, WYLD, and SYLD under the same rainfall conditions. These findings are consistent with the findings of Zhang et al. (2020), who reported that forest and agricultural land conversion to urban lands resulted in increased surface flow, decreased groundwater recharge, and greater sediment loss due to a reduction in impervious surfaces.

The WYLD and ET trends in S2 and S3, in which only climate change was investigated, were similar to S4 and S5, where both climate and land use changes were evaluated (Fig. 7). Thus, we conclude that WYLD and ET changes in different months are mostly due to climate change. Kundu et al. (2017) also concluded that climate change has a more profound impact on WYLD than land use change. However, the effect of land use change on WYLD is more discernible at the scale of the hydrological response unit than at the watershed level. Merz et al. (2009) suggested that the use of sub-basins to model larger basins generally provides a higher level of detail. Hence, different scales should be considered in planning and managing watersheds.

In this study, sub-basins 1 and 2 had the highest amount of WYLD in all scenarios. This increase is not only due to climate change but also to the conversion of a large part of good rangelands to barren land due to overgrazing by livestock and overharvesting of rangeland

348 plants. The transformation of rangelands to barren lands leads to an increase in WYLD.
349 These findings are in line with Chemura et al. (2020), who found that a reduction in
350 vegetation cover caused an increase in surface flow and a large increase in WYLD.

351 As previously mentioned, our results suggest that the effect of climate change on WYLD
352 is considerably stronger than land use change. A rise in WYLD is directly related to an
353 increase in precipitation and surface runoff. Thus, WYLD in RCP 4.5 was higher than in
354 RCP 8.5. Other studies have reported similar results. For example, Ndhlovu and Woyessa
355 (2020) reported higher rainfall, runoff, and WYLD in RCP 4.5 than in RCP 8.5. Likewise,
356 Nilawar and Waikar (2019) observed more precipitation, streamflow, and sediment
357 concentration in RCP 4.5 than in RCP 8.5.

358 Most Taleghan Catchment sub-basins had a higher WYLD in S2 than in S3 and in S4
359 than in S5 (Figs. 5 and 7). Most of the Taleghan Catchment is covered with sandy loam
360 soils with high erodibility (Hosseini and Ashraf, 2015). In the baseline scenario, SYLD was
361 less than 2 t/ha in all sub-basins (Fig. 6). However, the SWAT model results indicate that
362 land use change will lead to an almost elevenfold increase in SYLD by 2040. A comparison
363 between trends in different months shows lower SYLD in S2 and S3 than in S1 in all
364 months except May (Fig. 8). Also, SYLD increase in S1, in which only land use change
365 was examined, was considerably greater than in S2 and S3, where only climate change was
366 simulated.

367 Average annual SYLD in S1, S2, S3, S4, and S5 was 10, 5, 3, 14, and 11 times that of
368 the baseline scenario, respectively. Therefore, we conclude that the effect of land use
369 change on SYLD is significantly more powerful than that of climate change. However, the
370 combined impact of both is greater than that of land use change alone. Also, RCP 4.5 will
371 lead to a greater increase in SYLD than RCP 8.5. One of the most critical factors for SYLD
372 increase in an area like the Taleghan Catchment is vegetation loss. With decreased

vegetation, these areas will become more prone to water and wind erosion. Increased rainfall and reduced soil permeability will increase surface runoff. As a result, soil erosion and SYLD will increase. Yaa et al. (2012) also found that urbanization has expanded the impermeable surface area, increased the runoff coefficient, reduced the concentration time, and increased the peak flow and frequency of floods.

It is noteworthy that in all scenarios, precisely the sub-basins that had the highest WYLD, such as sub-basins 1, 2, 11, and 51, also had the highest SYLD. Kara et al. (2012) also reported a positive correlation between WYLD and SYLD in a small catchment in eastern Alabama, USA. Therefore, the sub-basins that are most susceptible to WYLD and SYLD changes can be predicted. This will facilitate water and soil planning and management in watersheds and help prioritize measures to improve them.

6 Conclusion

In this study, the separate and combined effects of climate and land use changes on WBCs on different spatial and temporal scales were analysed, with a focus on WYLD and SYLD. Six scenarios (one for the present and five for the future) were simulated. Our conclusions are as follows:

(1) According to the 2040 land use map obtained by the CA-Markov model, most land use changes are related to the conversion of rangelands to barren lands. Sub-basins 1, 2, 11, and 51, which show the highest SYLD, are the most vulnerable to sediment loss.

(2) In both RCP 4.5 and RCP 8.5, the highest SYLD value is in April and May in the spring and February in the winter.

(3) In the future, most WYLD will be produced in March, April, and May in spring and February in winter. In the summer, when the rainfall is negligible, WYLD and SYLD

will decrease precipitously. Sub-basins 33, 34, 43, 44, 45, 47, 48, 49, and 50 are the most vulnerable to WYLD changes.

(4) S4 shows the highest WYLD (295 mm) and SYLD (17t/ha).

(5) The effect of climate change on WYLD is stronger than that of land use change. Conversely, the effect of land use change on SYLD is greater than that of climate change. Their combined impacts on WYLD and SYLD are more profound than those of climate and land use changes separately.

Analyses of the combined effects of climate and land use change on different spatial and temporal scales can provide more accurate results than separate analyses. Planning and management strategies should take these results into account to prevent the deterioration of water and soil resources in watersheds, especially in such arid regions as Iran.

Acknowledgements

The first author would like to express her gratitude to Eawag for providing a fellowship through the Eawag Partnership Programme, which allowed her to conduct part of this research in Switzerland.

References

Abbaspour KC, Yang J, Maximov I, Siber R, Bogner K, Mieleitner J, Zobrist J, Srinivasan R. (2007). Modelling hydrology and water quality in the pre-alpine/alpine Thur watershed using SWAT. Journal of Hydrology 333:413-430.

Abbaspour KC, Vaghefi SA, Yang H, Srinivasan R (2019) Global soil, landuse, evapotranspiration, historical and future weather databases for SWAT applications. Nature Scientific Data 6:263.

Aparicio JS, Sáez PJ, Crespo AB, Sánchez JP, Velázquez OP (2019) Coupling machine-learning techniques with SWAT model for instantaneous peak flow prediction. Biosystems Engineering 177:67–77.

Arnold JG, Kiniry JR, Srinivasan R, Williams J R, Haney EB, Neitsch SL (2011) Soil and water assessment tool input-output file documentation. Soil and Water Research Laboratory, Grassland, 808 East Black Land Road, Temple, Texas.

Bazab Consulting Engineers (2015) Comprehensive environmental impact assessment studies of Taleghan reservoir dam and Sangban underground power plant. Tehran, Iran.

Boretti A, Rosa L (2019) Reassessing the projections of the World Water Development Report. npj Clean Water 2:15.
Chauhan N, Kumar V, Paliwal R (2020) Quantifying the impacts of decadal landuse change on the water balance components using soil and water assessment tool in Ghaggar river basin. SN Appl Sci 2:1777.
Chemura A, Rwasoka D, Mutanga O, Dube T, Mushore T (2020) The impact of land-use/land cover changes on water balance of the heterogeneous Buzi sub-catchment, Zimbabwe. Remote Sensing Applications: Society and Environment 18:100292.
Chen M, Gassman PM, Srinivasan R, Cui Y, Arritt R (2020) Analysis of alternative climate datasets and evapotranspiration methods for the upper Mississippi river basin using SWAT within HAWQS. Science of the Total Environment 720:137562.
Choukri F, Raclot D, Naimi M, Chikhaoui M, Pedro Nunes J, Huard F, Hérivaux C, Sabir M, Pépin Y (2020) Distinct and combined impacts of climate and land use scenarios on water availability and sediment loads for a water supply reservoir in northern Morocco. International Soil and Water Conservation Research, In Press.
Crosta AP, Moore JM (2007) Geological mapping using Landsat thematic mapper imagery in Almeria Province, South-east Spain. Int J Remote Sens 10:505–514.
Dibaba WT, Demissie TA, Miegel K (2020) Watershed hydrological response to combined land use/land cover and climate change in Highland Ethiopia: Finchaa catchment. Water 12:1801.
Dunne JP, John JG, Adcroft AJ, Griffies SM, Hallberg RW, Shevliakova E, Zadeh N (2012) Global coupled carbon–climate Earth System Models. Part I: physical formulation and baseline simulation characteristics. Journal of Climate 25:6646–6665.
Eastman JR (2015) TerrSet manual. Access. TerrSet Vers 18:1–390.
Gassman PW, Reyes MR, Green CH, Arnold JG (2007) The soil and water assessment tool: historical development, applications, and future research directions. Trans ASABE 50:1211–1250.
Gupta HV, Sorooshian S, Yapo PO (1999) Status of automatic calibration for hydrologic models: comparison with multilevel expert calibration. J Hydrol Eng 4:135–143.
Hosseini M, Ashraf M (2015) Application of the SWAT model for water components separation in Iran. Springer, New York.
Kara F, Loewenstein E, Kalin L (2012) Changes in sediment and water yield downstream on a small watershed. Ekoloji 21:30–37.
Karan SK, Samadder SR (2016) Accuracy of land use change detection using support vector machine and maximum likelihood techniques for open-cast coal mining areas. Environ Monit Assess 188:486.
Kundu S, Khare D, Mondal A (2017) Individual and combined impacts of future climate and land use changes on the water balance. Ecological Engineering 105:42–57.
Legates DR, McCabe GJ (1999) Evaluating the use of "goodness-of-fit" measures in hydrologic and hydroclimatic model validation. Water Resour Res 35:233–241.
LV Z, Zuo J, Rodriguez D (2020) Predicting of runoff using an optimized SWAT-ANN: a case study. Journal of Hydrology: Regional Studies 29:100688.
Merz R, Parajka J, Blöschl G (2009) Scale effects in conceptual hydrological modeling. Water Resour Res 45:W09405.
Nandi S, Reddy JM (2020) Spatiotemporal analysis of water balance components and their projected changes in near-future under climate change over Sina basin, India. Water Resour Manage 34: 2657–2675.
Nash JE, Sutcliffe JV (1970) River flow forecasting through conceptual models part I–a discussion of principles. J Hydrol 10:282–290.

Nasiri S, Ansari H, Ziaei AN (2020) Simulation of water balance equation components using SWAT model in Samalqan watershed (Iran). Arabian Journal of Geosciences 13:421.
Ndhlovu G, Woyessa Y (2020) Modelling impact of climate change on catchment water balance, Kabompo River in Zambezi river basin. Journal of Hydrology: Regional Studies 27:100650.
Ni X, Parajuli PB, Ouyang Y (2020) Assessing agriculture conservation practice impacts on groundwater levels at watershed scale. Water Resour Manage 34:1553–1566.
Nilawar AP, Waikar ML (2019) Impacts of climate change on streamflow and sediment concentration under RCP 4.5 and 8.5: A case study in Purna river basin, India. Science of the Total Environment 650:2685–2696.
Ning JC, Gao ZQ, Lu QS (2015) Runoff simulation using a modified SWAT model with spatially continuous HRUs. Environ Earth Sci 74:5895–5905.
Odeh T, Rodiger T, Geyer S, Schirmer M (2015) Hydrological modelling of a heterogeneous catchment using an integrated approach of remote sensing, a geographic information system and hydrologic response units: the case study of Wadi Zerka Ma'in catchment area, north east of the Dead Sea. Environmental Earth Sciences 73:3309–3326.
Ramteke G, Singh R, Chatterjee C (2020) assessing impacts of conservation measures on watershed hydrology using MIKE SHE model in the face of climate change. Water Resour Manage 34**:**4233–4252.
Schmalz B, Kruse M, Kiesel J, Müller F, Fohrer N (2016) Water-related ecosystem services in Western Siberian low land basins-analyzing and mapping spatial and seasonal effects on regulating services based on ecohydrological modelling results. Ecological Indicators 71:55–65.
Seyoum WM, Milewski AM, Durham MC (2015) Understanding the relative impacts of natural processes and human activities on the hydrology of the Central Rift Valley lakes, East Africa. Hydrol Process 29:4312–4324.
Shooshtari SH, Shayesteh K, Gholamalifard M, Azari M, Serrano-Notivoli R, López-Morenoe JI (2017) Impacts of future land cover and climate change on the water balance in northern Iran. Hydrological Sciences Journal 62:2655–2673.
Tian Y, Wang S, Bai X, Luo G, Xu Y (2016) Trade-offs among ecosystem services in a typical Karst watershed, SW China. Science of the Total Environment 566-567:1297-1308.
Uniyal B, Dietrich J, Vasilakos C, Tzoraki O (2020) Evaluation of SWAT simulated soil moisture at catchment scale by field measurements and Landsat derived indices. Agricultural Water Management 193:55–70.
Vaghefi S, Abbaspoor N, Kamali B, Abbaspour KC (2017) A toolkit for climate change analysis and pattern recognition for extreme weather conditions – Case study: California-Baja California Peninsula. Environmental Modelling & Software 96:181–198.
Verma AK, Garg PK, Prasad KH (2017) Sugarcane crop identification from LISS IV data using ISODATA, MLC, and indices based decision tree approach. Arab J Geosci 10:16.
Vuuren DP, Edmonds J, Kainuma MLT et al. (2011) Representative concentration pathways: An overview. Clim Chang 109:5–31.
Wilken F, Wagner PD, Narasimhan B, Fiener P (2017) Spatio-temporal patterns of land use and cropping frequency in a tropical catchment of South India. Applied Geography 89:124–132.
Williams J R (1975) Sediment routing for agricultural watersheds. Water Resour Bull 11:965–974.
Willmott CJ (1984) On the evaluation of model performance in physical geography. Springer, New York.
Yaa L, Youpeng X, Yi S (2012) Hydrological effects of urbanization in the Qinhuai River Basin, China. Procedia Eng 28:767–771.

Zhang H, Wang B, Liu DL, Zhang M, Leslie LM, Yu Q (2020) Using an improved SWAT model to simulate hydrological responses to land use change: A case study of a catchment in tropical Australia. Journal of Hydrology 585:124822.

Zheng Y, Zhang M, Wu (2016) Using high spatial and temporal resolution data blended from SPOT-5 and MODIS to map biomass of summer maize. In: Fifth International Conference on Agro-Geoinformatics, Tianjin.

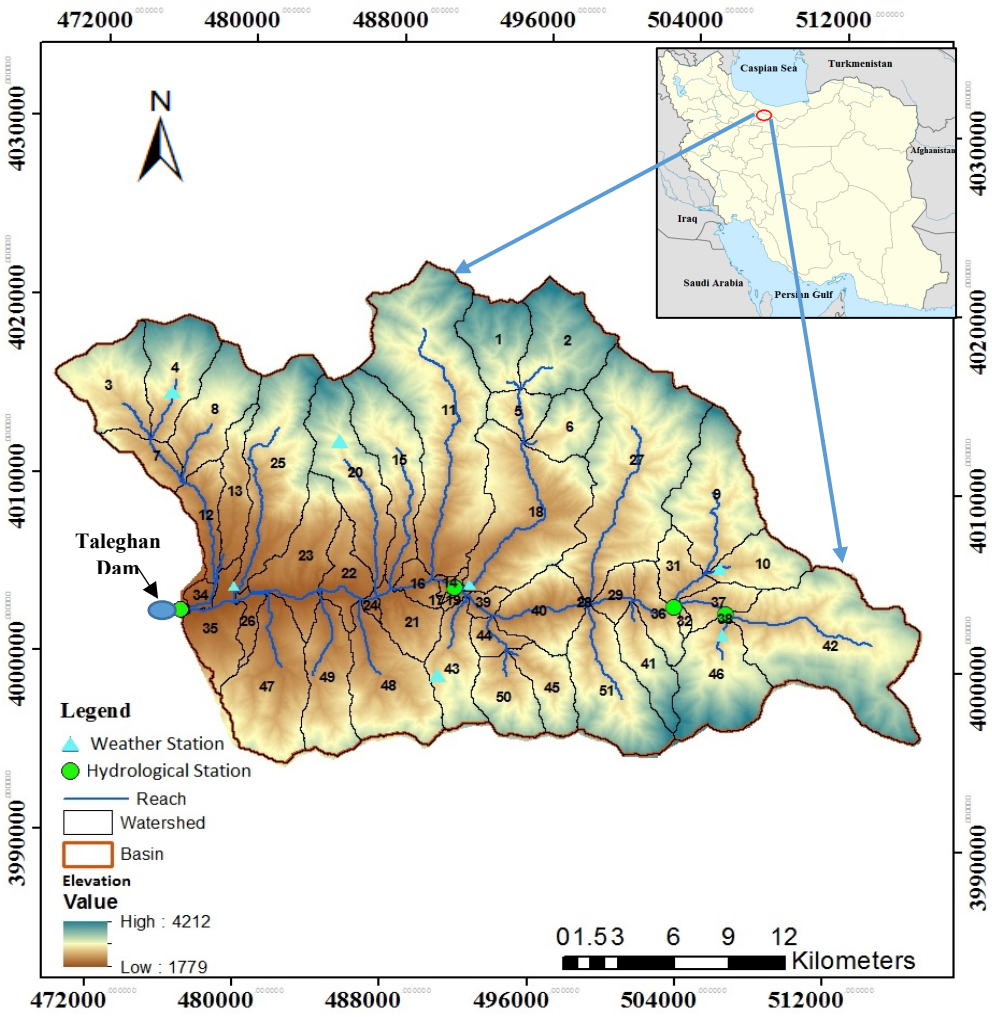

Fig. 1 Location of the Taleghan Catchment in Iran

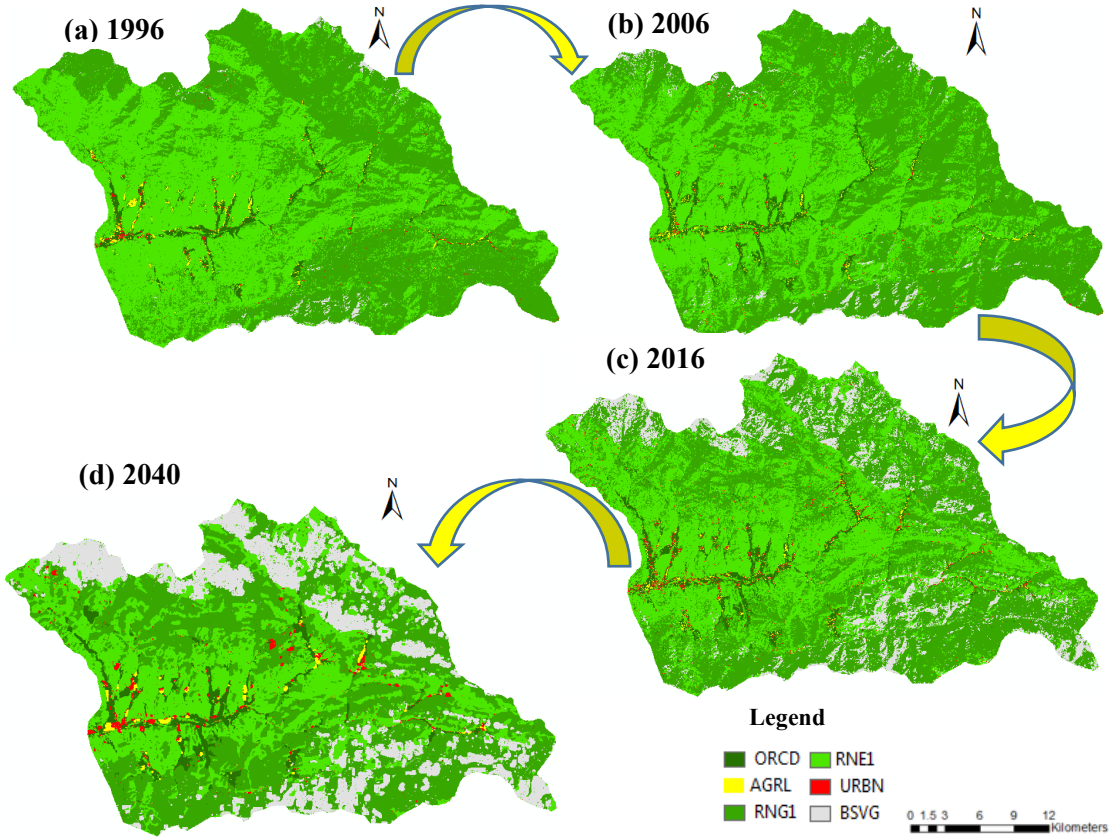

Fig. 2 Land use maps for 1996, 2006, 2016, and 2040 (ORCD: orchard, AGRL: agricultural land, RNG1: good rangeland, RNE1: poor rangeland, URBN: urban areas, BSVG: barren land or wasteland)

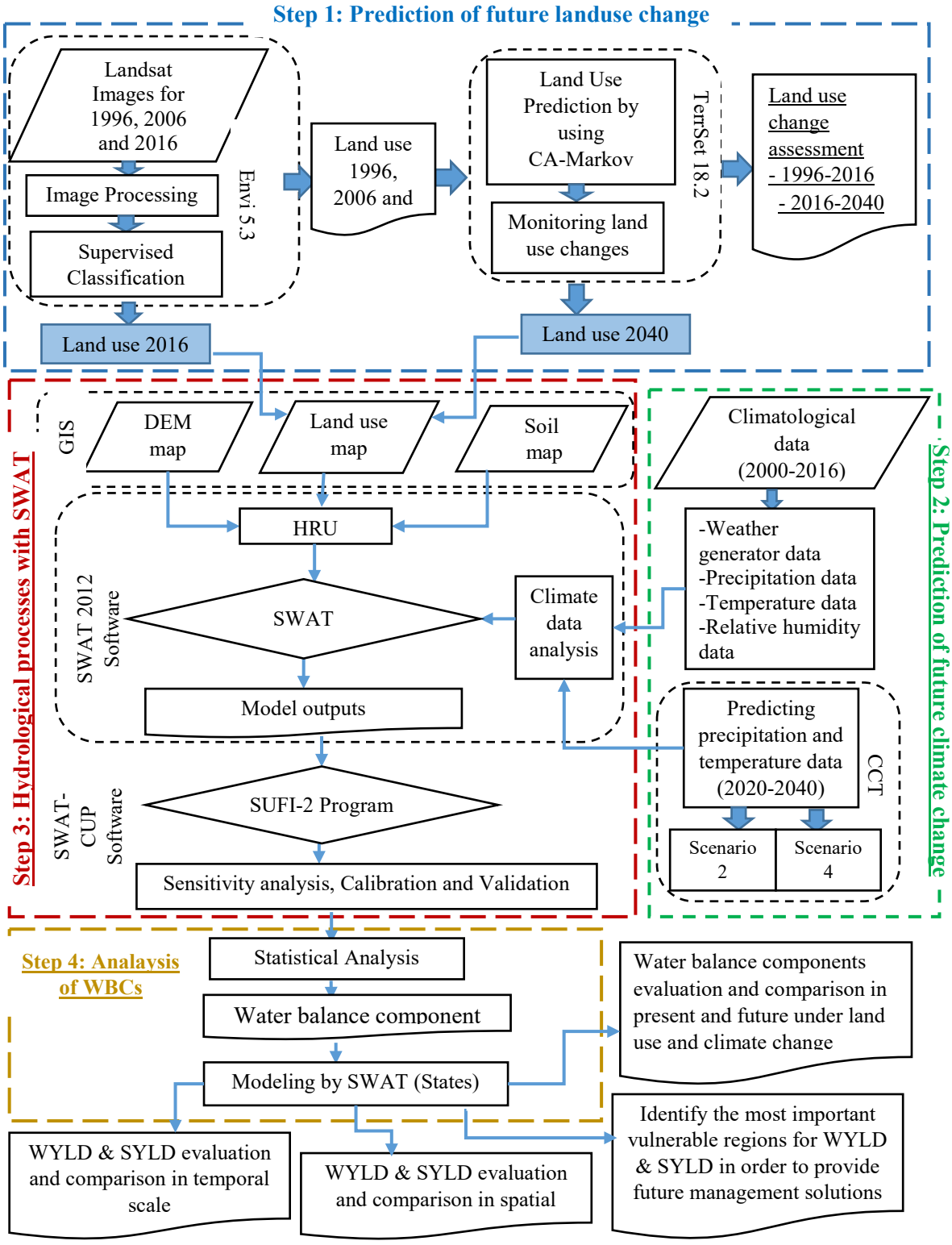

Fig. 3 Framework of the methodology

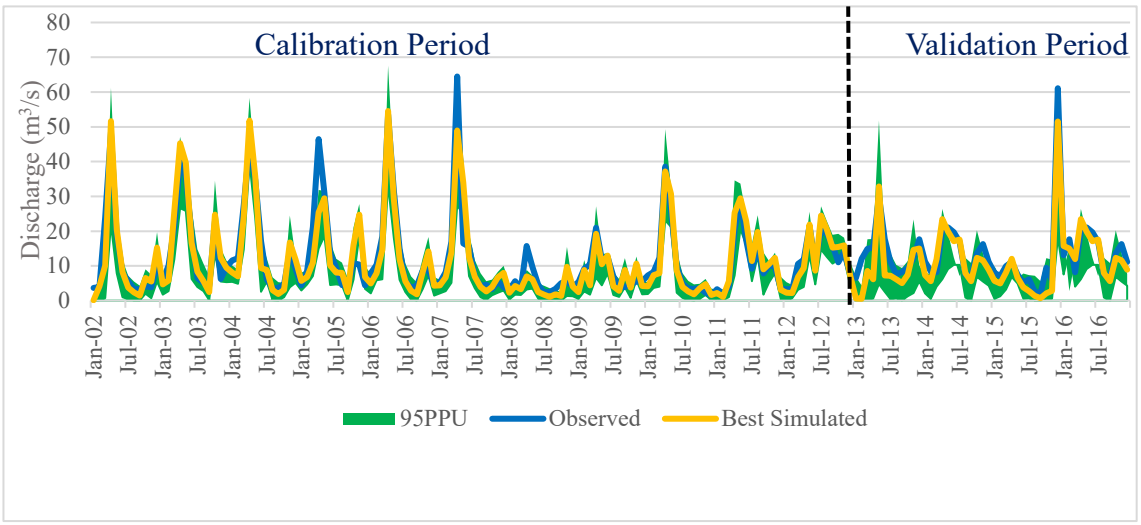

Fig. 4 Observed and best simulated monthly runoff for calibration, validation, and 95% prediction uncertainty (95PPU) at the Galinak station

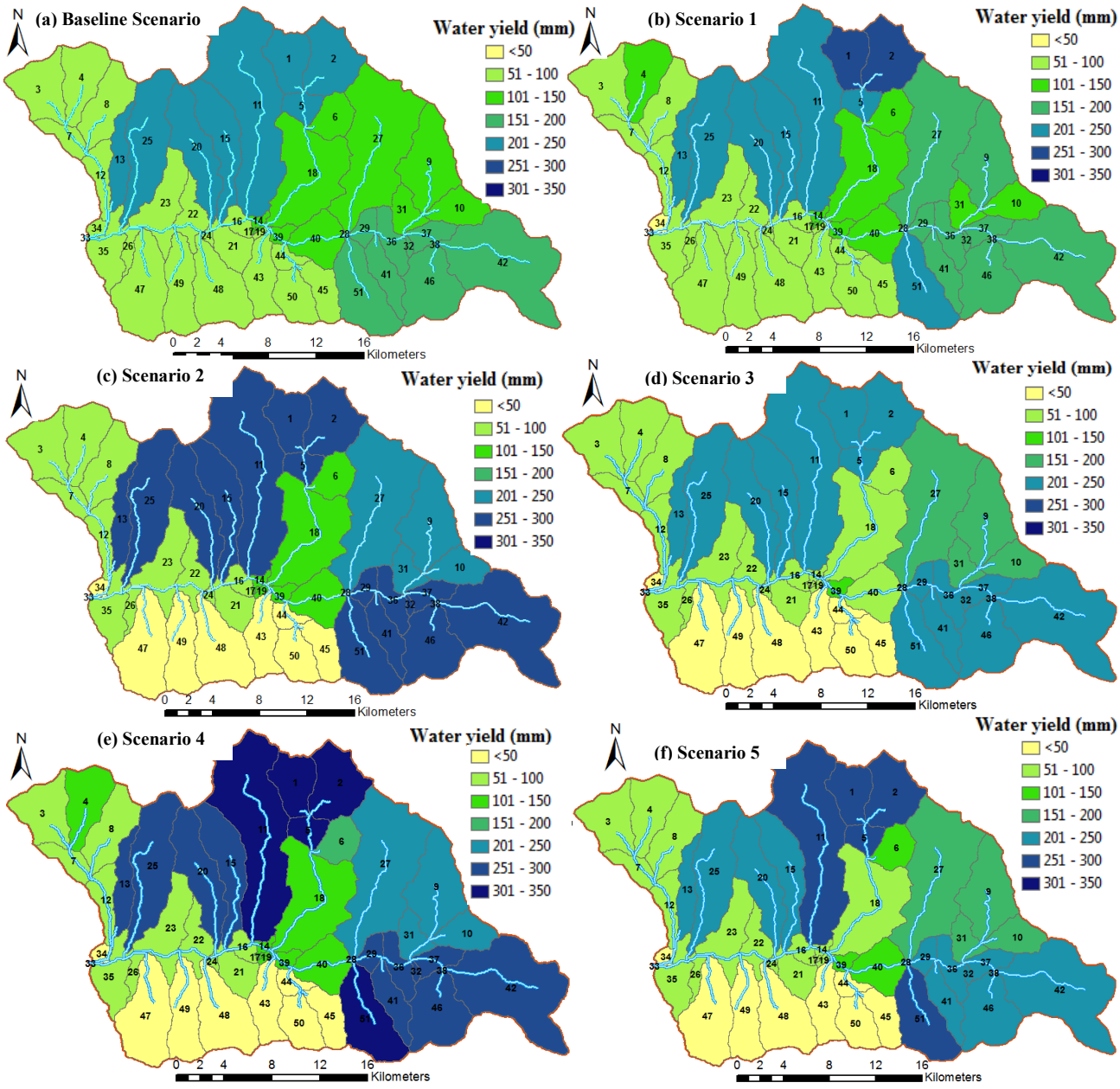

Fig. 5 Average annual WYLD in the sub-basins

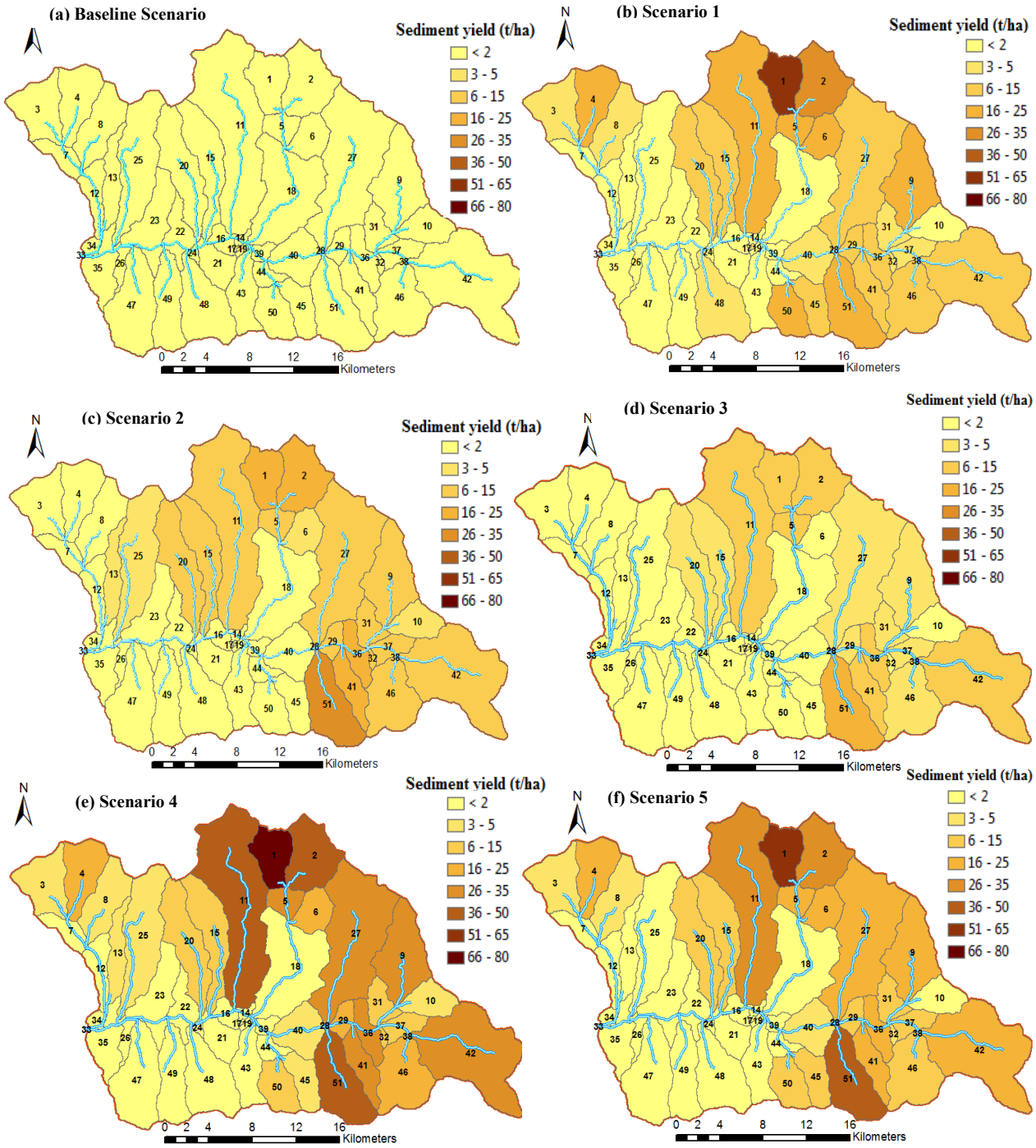

Fig. 6 Average annual SYLD in the sub-basins

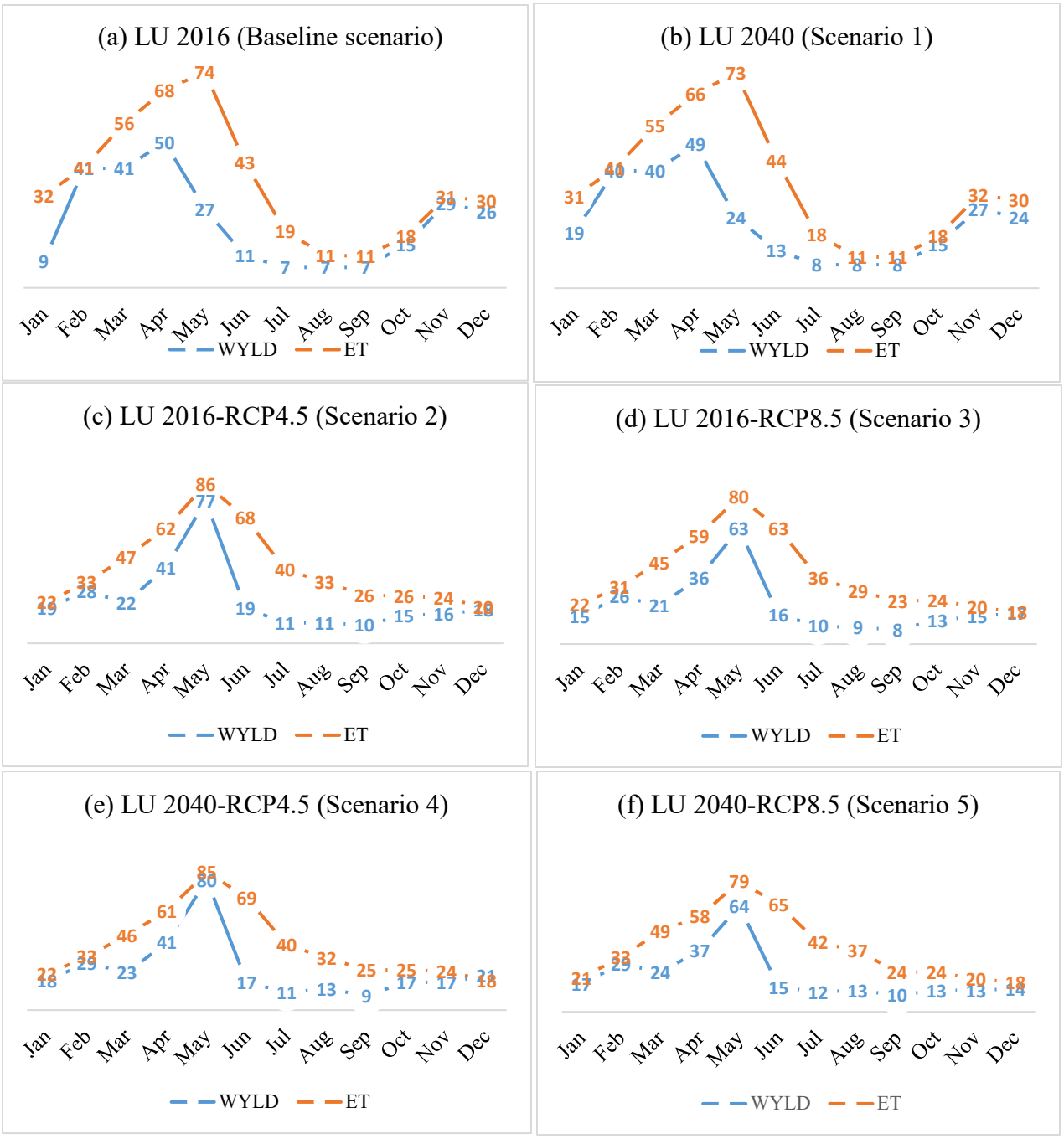

Fig. 7 Average monthly WYLD for the period of 2000-2016 for a) baseline scenario and b) scenario 1 and 2020-2040 for c) scenario 2, d) scenario 3, e) scenario 4, and f) scenario 5

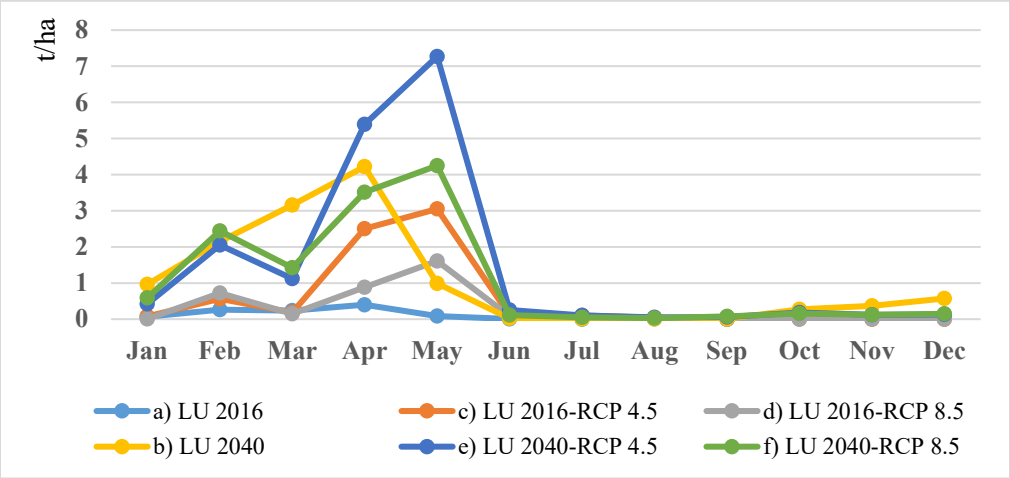

Fig. 8 Average monthly SYLD for the period of 2000-2016 for a) baseline scenario and b) scenario 1 and 2020-2040 for c) scenario 2, d) scenario 3, e) scenario 4, and f) scenario 5

Table 1 Data type and sources used in the SWAT model

Data type	Resolution	Source
Digital elevation model (DEM)	30 m	Iran National Cartographic Center (INCC) map http://www.ncc.ir
Soil map (texture, depth, and drainage attributes)	5 km Rasterized to a 30 m grid size and three classes	FAO–UNESCO global soil map (Abbaspour et al., 2019)
Landuse map	30 m	https://earthexplorer.usgs.gov/
Climate data (daily precipitation, min/max temperature, humidity, wind speed, and solar radiation during 2000-2016)	7 stations	Iran Meteorological Organization http://www.irimo.ir
Hydrological data (monthly river discharge during 2000-2016)	4 stations	Iran Water Resources Management Company http://www.wrm.ir
Sediment data (monthly sediment, during 2000-2016)	4 stations	Iran Water Resources Management Company http://www.wrm.ir

Table 2 The percentage area of land use classes

Land use	Area (%)				Percent of Change	
	1996	2006	2016	2040	(1996-2016)	(2016-2040)
Orchard	2.06	2.43	3.41	4.34	1.35	0.93
Agricultural land	0.60	0.38	0.37	0.56	-0.23	0.19
Good rangeland	47.81	54.16	47.49	43.02	-0.32	-4.47
Poor rangeland	48.55	41.28	38.31	32.93	-10.24	-5.38
Urban areas	0.28	0.28	0.92	1.32	0.64	0.4
Barren land	0.70	1.47	9.50	17.83	8.8	8.33
Total	100	100	100	100	-	-

Table 3 Coefficients for assessing the model performance

Period	Hydrological station	R*	NSE**	RSR***	PBIAS**** (%)
Calibration (2000-2012)	Gatedeh	0.92	0.90	0.31	-8.9
	Dehdar	0.91	0.90	0.31	3.0
	Joestan	0.89	0.84	0.40	-3.0
	Galinak	0.86	0.85	0.39	2.9
Validation (2013-2016)	Gatedeh	0.77	0.69	0.55	-2.3
	Dehdar	0.77	0.63	0.61	-11.6
	Joestan	0.87	0.75	0.50	24.2
	Galinak	0.87	0.80	0.45	19.7

*R2: Coefficient of determination

**NSE: Nash–Sutcliffe Efficiency

***RSR: RMSE-Observations Standard Deviation Ratio

****PBIAS: Percent bias

Table 4 Average annual water balance components in the Taleghan Catchment

Variable	Baseline scenario	Landuse change	Climate change		Landuse and climate changes	
		Scenario 1	Scenario 2	Scenario 3	Scenario 4	Scenario 5
Precipitation (mm)	629	629 (0%)	717 (14%)	641 (2%)	717 (14%)	641 (2%)
Evapotranspiration (mm)	358	353 (-1%)	429 (20%)	392 (9%)	422 (18%)	380 (6%)
Surface runoff (mm)	99	116 (17%)	104 (5%)	86 (-13%)	124 (26%)	110 (11%)
Groundwater flow (mm)	65	58 (-11%)	70 (7%)	59 (-9%)	61 (-7%)	52 (-21%)
Lateral flow (mm)	106	101 (-5%)	114 (7%)	103 (-3%)	111 (4%)	99 (-7%)
Revap (mm)	34	31 (-10%)	34 (0%)	31 (-8%)	31 (-10%)	28 (-19%)
WYLD (mm)	270	275 (2%)	288 (7%)	248 (-8%)	295 (9%)	260 (-4%)
SYLD (t/ha)	1.2	12.7 (948%)	6.7 (447%)	3.6 (191%)	17 (1312%)	12.9 (961%)